

SUPPORTING INFORMATION

Extended and functionalized porous iron(III) tri- or dicarboxylates with MIL-100/101 topologies

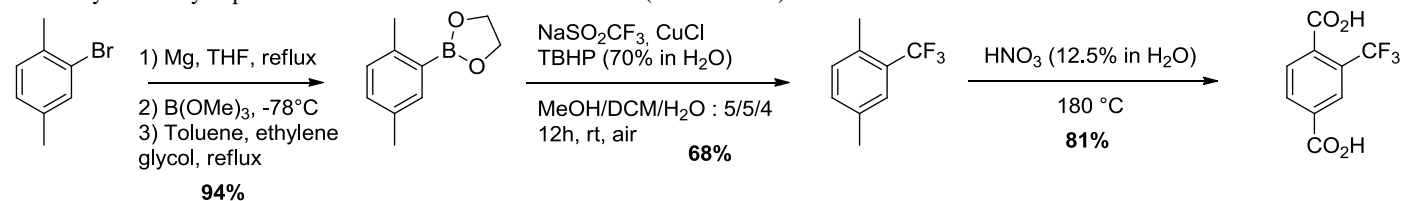
Patricia Horcajada,^{*a} Hubert Chevreau,^{a,d} Daniela Heurtaux,^a Farah Benyettou,^a Fabrice Salles,^b Thomas Devic,^a Alfonso Garcia-Marquez,^a Cihang Yu,^a Hubert Lavrard,^a Claire L. Dutson,^a Emmanuel Magnier,^a Guillaume Maurin,^b Erik Elkaïm,^c Christian Serre ^{*a}

1. SYNTHESIS

N,N-dimethylformamide (DMF 99%, acetone (99%), absolute ethanol and hydrochloric acid (37%) were purchased from Carlo Erba. Methanol (99.9%) and nitric acid (70%) were purchased from VWR Switzerland. All the solvents were used as purchased. Iron(III) chloride hexahydrate and hydrofluoric acid (HF, 40%) were obtained from Alfa Aesar. Iron(III) perchlorate (99%), terephthalic acid (BDC), 2-aminoterephthalic acid (NH₂-BDC), 2-bromoterephthalic acid (Br-BDC, 99 %), 4,4'-biphenyldicarboxylic acid (BPDC, 98%) and 2,6-naphthalenedicarboxylic acid (99%) were purchased from Sigma-Aldrich. All the chemicals were used without further purification.

Organic ligands:

2,5-dimethylterephthalic acid (2CH₃-H₂BDC)¹ and 2-chloroterephthalic acid (Cl-H₂BDC) were synthesized according to literature.² 2-(trifluoromethyl)terephthalic acid (CF₃-H₂BDC) was synthesized in a three-steps procedure starting from commercially available 2-bromo-*p*-xylene which was transformed into a borolane. The trifluoromethyl group was then introduced according to the Sanford³ procedure and lastly the benzylic positions oxidized under acidic conditions (see scheme 1).



Scheme 1. Synthetic scheme of 2-(trifluoromethyl)terephthalic acid

2-(2,5-dimethylphenyl)-1,3,2-dioxaborolane: under an argon atmosphere, magnesium powder (1.55 g, 64.0 mmol, 50 mesh) were covered with dry THF (80 mL). 2-bromo-1,4-dimethylbenzene (8.0 mL, 58.0 mmol) was added dropwise, and the solution was therefore refluxed. After 1h30, the dark solution was cooled down, and added dropwise into a solution of trimethyl borate (12.9 mL, 116 mmol) in dry THF (80 mL), at -78°C. The greyish solution was warmed to room temperature, and concentrated to dryness by rotary evaporator. To the resulting solid were added ethylene glycol (26 mL) and toluene (80 mL). The mixture was refluxed overnight, and the toluene layer was separated and concentrated to dryness by rotary evaporator (3h, 70°C, 50 mbar) to afford the product as a turbid liquid (9.65 g, 94%), used without further purification. ¹H NMR (CDCl₃, 300 MHz): δ 7.68 (bs, 1H), 7.21 (dd, J=7.7; 1.6 Hz, 1H), 7.13 (d, J=7.8 Hz, 1H), 4.39 (s, 4H), 2.56 (s, 3H), 2.36 (s, 3H); ¹³C NMR (CDCl₃, 75 MHz): δ 141.7, 136.8, 133.6, 131.7, 129.7, 65.4, 21.6, 20.5

1,4-dimethyl-2-trifluoromethyl-benzene: to a solution of 2-(2,5-dimethylphenyl)-1,3,2-dioxaborolane (9.0 g, 51.2 mmol), CuCl (5.06 g, 51.2 mmol), and NaSO₂CF₃ (23.94 g, 153.4 mmol) in a mixture of DCM/MeOH/H₂O (102 mL/102 mL/84 mL) at 0°C, *tert*-butyl hydroperoxide (70% w/w in water, 31.0 mL, 256 mmol) was added dropwise. The reaction was allowed to warm to room temperature and stirred for 12h. Diethyl ether (200 mL) was added. The organic layer was washed with saturated aqueous sodium bicarbonate (300 mL) and potassium sulfite (200 mL) solutions, dried over MgSO₄ and concentrated under reduced pressure. The crude mixture was purified by flash chromatography on silica gel to afford the title compound (6.04 g, 68%) as a colorless liquid. ¹H NMR (CDCl₃, 200 MHz): δ 7.4 (s, 1H), 7.2 (AB system, 2H), 2.45 (s, 3H), 2.4 (s, 3H); ¹⁹F NMR (CDCl₃, 188 MHz): δ -62.14 (3F, CF₃).

2-(trifluoromethyl)terephthalic acid: a Teflon lined vessel (125 ml) was charged with 1,4-dimethyl-2-trifluoromethyl-benzene (2.7 g, 15.5 mmol), water (30 mL) and nitric acid (50%, 15 mL). The vessel was sealed and heated at 180 °C for 24 hrs. The resulting solid was collected by filtration and washed with water to afford the desired compound as a white solid (3.0 g, 81 %). ¹H NMR (200 MHz, DMSO): δ 8.25 (m, 1H), 8.24 (m, 1H), 7.93 (m, 1H); ¹⁹F NMR (188 MHz, DMSO): δ -61.66 (3F, CF₃); HRMS (EI): m/z [M-H]⁺ calcd for C₉H₅F₃O₄: 233.0062; found : 233.0065.

Metal-Organic Frameworks:

The microwave-assisted hydro/solvothermal syntheses were performed in a MARS-CEM® (North Carolina, USA, 1600 W) microwave oven.

Classical solvothermal-syntheses were performed in Heraeus Instruments Function line® (Germany) ovens using individual Teflon lined Parr-type metal autoclaves.

Iron terephthalate or MIL-101(Fe)-BDC

Synthesis: 270 mg (1 mmol) of FeCl₃·6H₂O (Aldrich, 99%) and 249 mg (1.5 mmol) of terephthalic acid (Aldrich, 98%) were dispersed in 15 mL of DMF, 20 μL of a 4 M hydrofluoric acid solution were therefore added. The mixture was placed into a Teflon-lined autoclave (23 mL) and heated at 100°C for 16 hours. Then, the orange solid was recovered by filtration and washed with DMF.

Activation: 150 mg of crude MIL-101(Fe)-BDC were suspended in 10 mL of DMF and centrifuged during 30 minutes at 10500 rpm/min. Then MIL-101(Fe)-BDC was suspended in 25 mL of ethanol and centrifuged during 30 minutes at 10500 rpm/min. The previous sequence was repeated 10 times.

Iron 2,5-dimethylterephthalate or MIL-101(Fe)-2CH₃

Synthesis: 354 mg (1 mmol) of Fe(ClO₄)₃·nH₂O and 194 mg (1 mmol) of 2,5-dimethylterephthalic acid were dispersed in 5 mL of DMF. The mixture was placed into a 23 mL Teflon-lined autoclave and heated at 150 °C for 15 hours. The reaction mixture was centrifuged (10500 rpm/min); the solid was recovered and washed with ethanol.

Activation: 150 mg of crude MIL-101(Fe)-2CH₃ were suspended in 25 mL of ethanol and centrifuged during 30 minutes at 10500 rpm/min. The sequence was repeated 10 times.

Iron 2-aminoterephthalate or MIL-101(Fe)-NH₂

Synthesis: 135 mg (0.5 mmol) of FeCl₃·6H₂O and 90.5 mg (0.5 mmol) of 2-aminoterephthalic acid were dispersed in 25 mL of deionized water. The mixture was placed into a 100 mL Teflon-lined autoclave. The reactor was heated under microwave irradiation at 100 °C (600 W) for 5 minutes. The resulting suspension was cooled down and centrifuged at 10500 rpm for 25 min. The solid was recovered and washed with absolute ethanol.

Activation: 40 mg of crude MIL-101(Fe)-NH₂ were suspended in 25 mL of ethanol and centrifuged during 30 minutes at 10500 rpm/min. The action was repeated 5 times, obtaining the MIL-101(Fe)-NH₂.

Iron 2-chloroterephthalate or MIL-101(Fe)-Cl

Synthesis: 270 mg (1 mmol) of FeCl₃·6H₂O and 200 mg (1 mmol) of 2-chloroterephthalic acid were dispersed in 5 mL of DMF. 0.4 mL of a 2 M sodium hydroxide solution were subsequently added. The mixture was placed into a round-bottomed flask and heated at 100 °C for 2 hours. The obtained solid was recovered by centrifugation and washed with ethanol.

Activation: 200 mg of crude MIL-101(Fe)-Cl were suspended in 25 mL of absolute ethanol and centrifuged during 30 minutes at 10500 rpm/min. The sequence was repeated 10 times.

Iron 2-bromoterephthalate or MIL-101(Fe)-Br

Synthesis: 270 mg (1 mmol) of FeCl₃·6H₂O and 270 mg (1 mmol) of 2-bromoterephthalic acid were dispersed in 10 mL of DMF. The mixture was placed in a round-bottomed flask and heated at 100 °C for 16 hours. The obtained solid was recovered by centrifugation.

Activation: 200 mg of crude MIL-101(Fe)-Br were suspended in 25 mL of absolute ethanol and centrifuged during 30 minutes at 10500 rpm/min. The exchange was repeated 10 times.

Iron 2-(trifluoromethyl)terephthalate or MIL-101(Fe)-CF₃

Synthesis: 675 mg (2.5 mmol) of FeCl₃·6H₂O and 585 mg (2.5 mmol) of 2-trifluoromethylterephthalic acid were dispersed in 25 mL of absolute ethanol into a Teflon-lined autoclave. The reactive mixture was heated under microwave irradiation at 100 °C (600 W) during 5 minutes. The resulting solid was recovered by centrifugation and washed with ethanol.

Activation: 200 mg of crude MIL-101(Fe)-CF₃ were suspended in 25 mL of ethanol and centrifuged during 30 minutes at 10500 rpm/min. The sequence was repeated 5 times.

Iron 2,6-naphthalendicarboxylate or MIL-101(Fe)-NDC

Synthesis: 53 mg (0.15 mmol) of Fe(ClO₄)₃·nH₂O (Aldrich, 99%) and 32.5 mg (0.15 mmol) of 2,6 naphthalendicarboxylic acid were dispersed in 15 mL of DMF and 20 μL of HF 5 M into a Teflon-lined autoclave (23 mL). The mixture was heated at 100 °C for 16 hours. The resulting mixture was poured into a FEP centrifuge tube and cooled down into an ice bath and centrifuged at 10500 rpm for 30 min, the solid was recovered by centrifugation and washed with DMF.

Activation: 30 mg of crude MIL-101(Fe)-BPDC were suspended in 25 mL of DMF and centrifuged during 30 minutes at 10500 rpm/min. The action was repeated 10 times, obtaining the MIL-101(Fe)-NDC.

Iron 4,4'-biphenyldicarboxylate or MIL-101(Fe)-BPDC

Synthesis: 53 mg (0.15 mmol) of Fe(ClO₄)₃·nH₂O and 36 mg (0.15 mmol) of 4,4'-biphenyldicarboxylic acid were dispersed in 15 mL of DMF into a Teflon-lined autoclave (23 mL), 20 μL of a 5 M HF solution were subsequently added. The reacting mixture was heated at 100°C for 16 hours. The resulting suspension was poured into a fluorinated ethylene propylene (FEP) centrifuge tube, cooled down into an ice bath and centrifuged at 10500 rpm for 25 min. The solid was recovered and washed with DMF.

Activation: 30 mg of crude MIL-101(Fe)-BPDC were suspended in 25 mL of DMF and centrifuged during 30 minutes at 10500 rpm. The sequence is repeated 10 times, obtaining the MIL-101(Fe)-BPDC.

Iron 1,3,5-benzene trisbenzoate or MIL-100(Fe)-BTB

Synthesis: 1 mmol of iron(III) chloride hexahydrate FeCl₃·6H₂O (270 mg) and 0.7 mmol of 1,3,5-benzenetrisbenzoate (300 mg) were dispersed in 4 mL of DMF. The mixture was introduced in a 25 mL Teflon vessel then sealed in a metallic Paar bomb and heated in 1 hour at 100°C and let 10 h at the same temperature. The resulting solid was washed twice with 20 mL of DMF.

Activation: 50 mg of crude MIL-100(Fe)-BT were suspended in 25 mL of DMF and centrifuged during 30 minutes at 10500 rpm/min. The action was repeated 10 times, obtaining the MIL-100(Fe)-BTB.

2. CHARACTERIZATION TECHNIQUES.

The particle size and zeta potential were measured using a Malvern Instruments Zetasizer Nano series Nano-ZS®. The nanoparticles were dispersed using a Branson Digital Sonifier® (Connecticut, USA, 400 W) at 10% of amplitude for 1 minute.

Transmission electron microscopy (TEM) images were collected in a Darwin 208 Philips microscope (60-80-100 KV; Camera AMT).

Nitrogen sorption studies were performed at 77 K on a Belsorp Max® porosimeter (BEL Japan Inc.). Prior to the sorption study, the samples were degassed under secondary vacuum and heated at 150 °C for 3 h.

Approximately 5-10 mg of samples was used for thermogravimetric analysis (TGA). Samples were analyzed under an oxygen flow (20 mL·min⁻¹) using a Perkin Elmer Diamond TGA/DTA STA 6000 (Connecticut, USA) running from room temperature to 600 °C with a scan rate of 3 °C·min⁻¹.

A small amount of solids was analyzed by a Thermo Nicolet spectrometer (Thermo, USA). The spectrum was recorded from 4000-400 cm⁻¹.

Synchrotron powder diffraction experiment has been carried out for pattern matching of the MIL-100/101 solids at the Cristal beamline, Soleil Synchrotron (Gif-sur-Yvette, France). A monochromatic beam was extracted from the U20 undulator beam by means of a Si(111) double monochromator. Its wavelength of 0.79024 Å was refined from a LaB6 (NIST Standard Reference Material 660a) powder diagram recorded just before the experiment. High angular resolution is obtained with, in the diffracted beam, a 21 perfect crystals Si(111) multi-analyzer similar to the one employed on beamline ID31 at ESRF.⁴ The wet sample is loaded in a 1.0 mm capillary (Borokapillaren, GLAS, Schönwalde, Germany) mounted on a spinner rotating at about 5 Hz to improve particles statistics. Diffraction data were collected in less than two hours in continuous scanning mode and the diffractogram is obtained from the precise superposition and addition of the 21 channels data. The XRPD patterns have been indexed using the indexing program Dicvol⁵, the Le Bail intensity extraction using the Fullprof suite⁶ and the Rietveld refinement using TOPAS 4.2.⁷

The stability of MOFs in different solvents was evaluated as follows. The solid sample was dispersed in the selected solvent and the mixture was readily injected into a glass capillary (diameter: 1.0 mm). The loaded capillary was then centrifuged at 1500 rpm during 3 minutes. The liquid on the upper part was removed and the capillary was sealed before the measurement. X ray powder diffraction (XRPD) patterns were recorded using a Bruker D8 powder diffractometer equipped with a Lynx-eye detector. Data collection was performed at room temperature in Debye–Scherrer geometry, with 2θ of 2–20°, with a 0.02° step width and using monochromated radiation with a wavelength of 1.5409Å. Data interpretation was completed using Dicvol program.⁵

2.1 FTIR

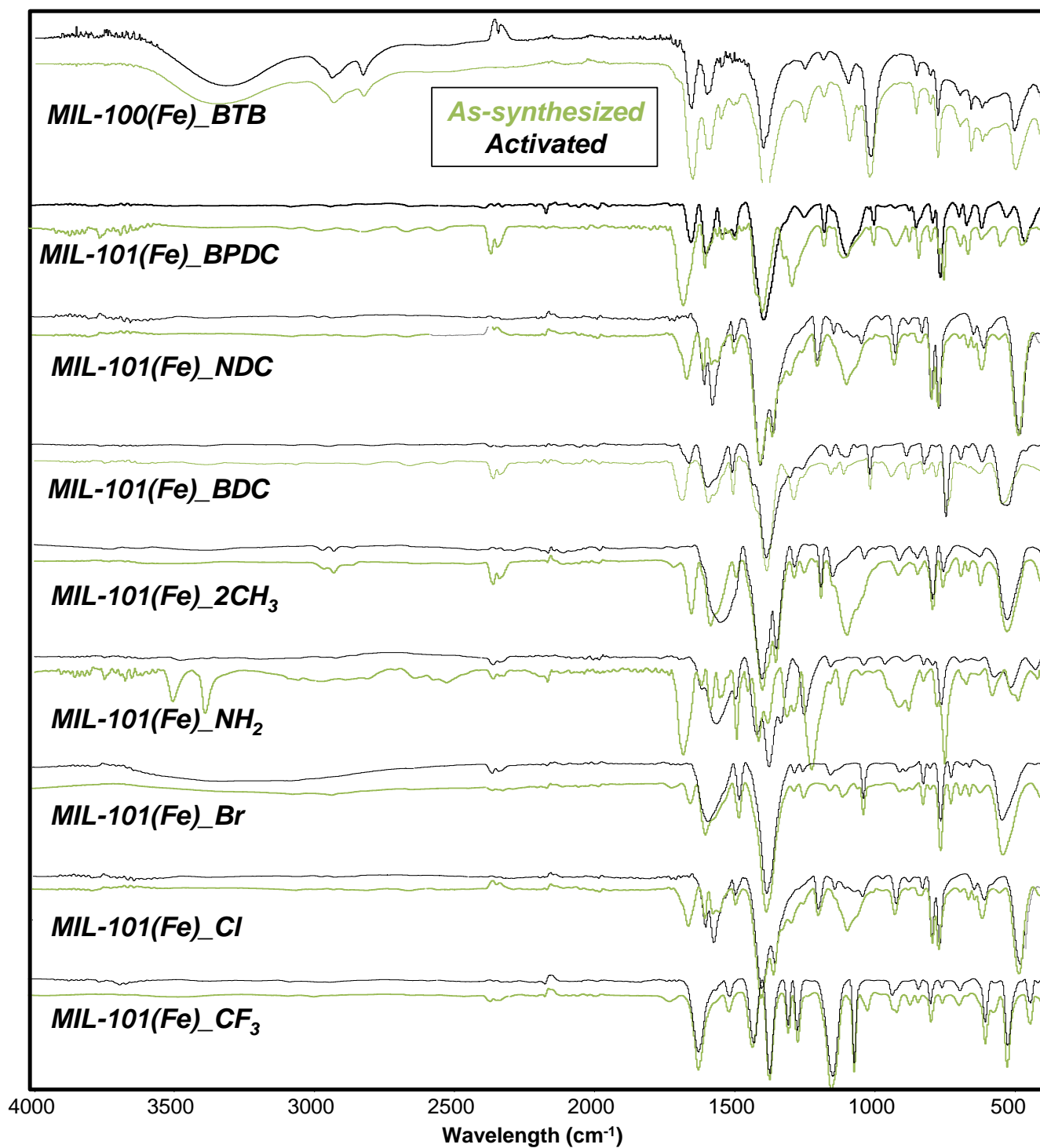


Figure S1. IR spectra of the as-synthesized (green) and activated (black) MIL100/MIL-101(Fe)_X nanoparticles.

2.2 XRPD

2.2.1 XRPD of MIL-100(Fe)_BTB and the series of MIL-101(Fe)

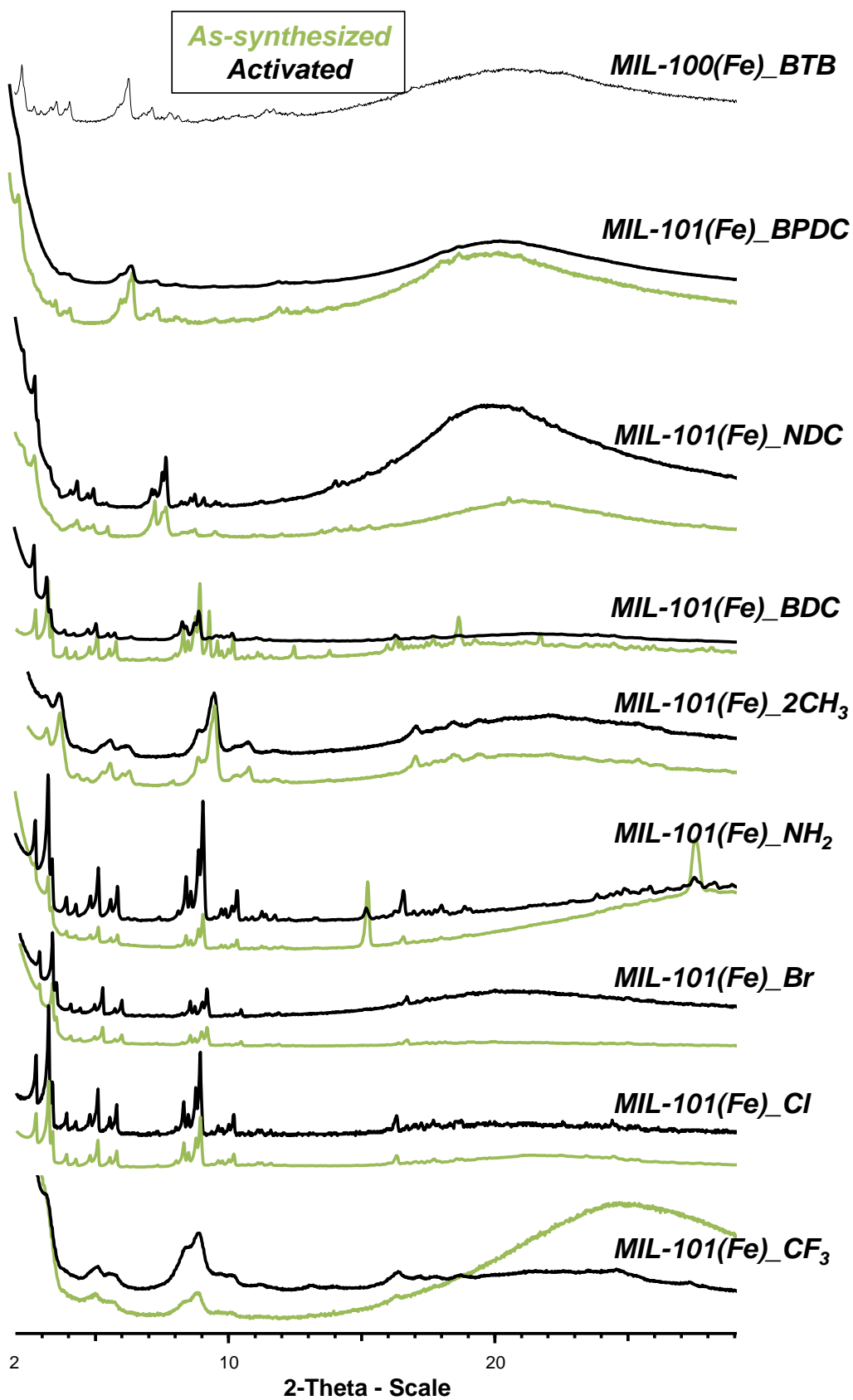


Figure S2. XRPD patterns of the as-synthesized (grey) and activated (black) MIL-100(Fe)_BTB and the series of MIL-101(Fe) solids.

2.2.2 Rietveld refinement of MIL-100(Fe)_BTB and MIL-101(Fe)_BPDC

XRPD data were collected at the SOLEIL synchrotron. First, a Le Bail intensity extraction using the program TOPAS 4.2⁷ was performed in order to extract the cell parameters and also to confirm the space group. Then, starting from this information, the structures were determined by simulation-assisted method using Materials Studio software.¹⁰ (details of the procedure are provided in the “computing simulation” part (2.6)). The so-obtained structures were thus used for Rietveld refinement, only the iron (Fe) and oxygens (O) were let free to refine and treated as isotropic, soft distance restrains were used to maintain the trimer-based inorganic unit. In both cases, the synchrotron XRPD measurements were carried out on solids containing solvents within the pores, the latest being difficult to precisely locate were replaced by oxygen atoms using Fourier map difference. The Rietveld refinement of MIL-100(Fe)_BTB is displayed in Fig. S3 and MIL-101(Fe)_BPDC in Fig. S4.

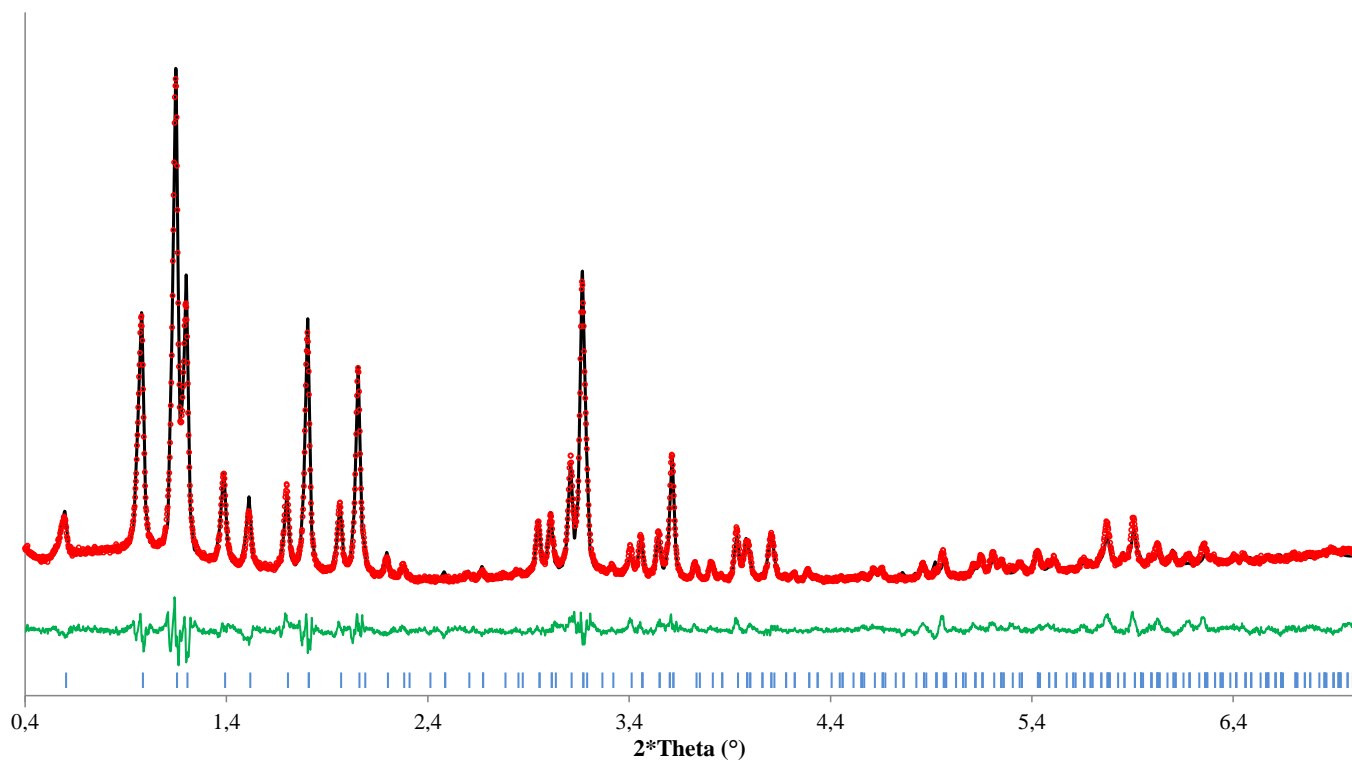


Figure S3. Rietveld refinement of MIL-100(Fe)_BTB in DMF ($Fd-3m$ ($n^{\circ}227$), $a = 130.035(6)$ Rwp=4.72%). ($\lambda = 0.79024\text{\AA}$)

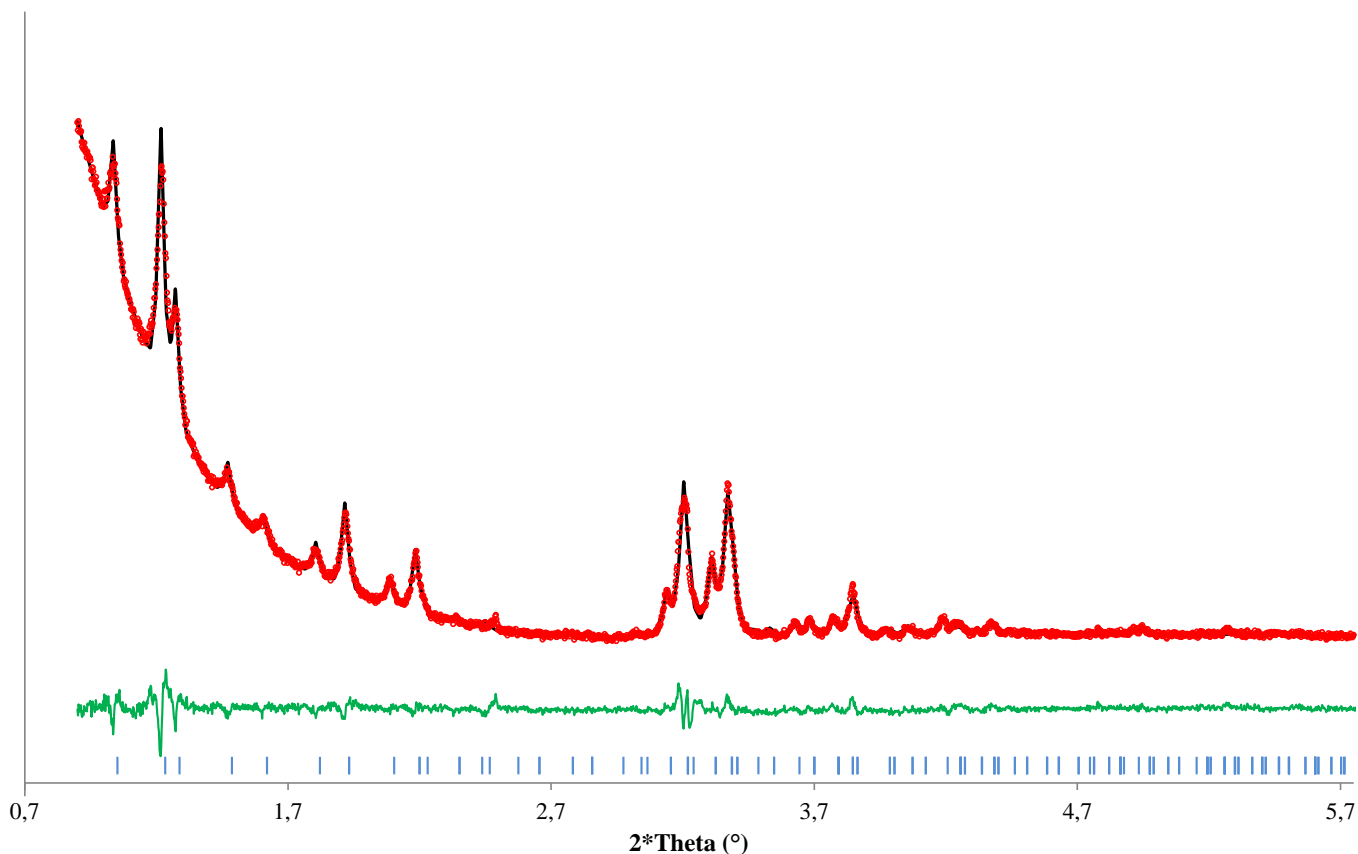


Figure S4. Rietveld refinement of MIL-101(Fe)_BPDC in DMF (*Fd-3* (*n*^o203), *a* = 121.809 (2) Rwp = 3.29%). ($\lambda = 0.79024\text{\AA}$)

2.2.3 Leball intensity extraction of MIL-101(Fe) (BDC, NDC and BPDC) in different solvents.

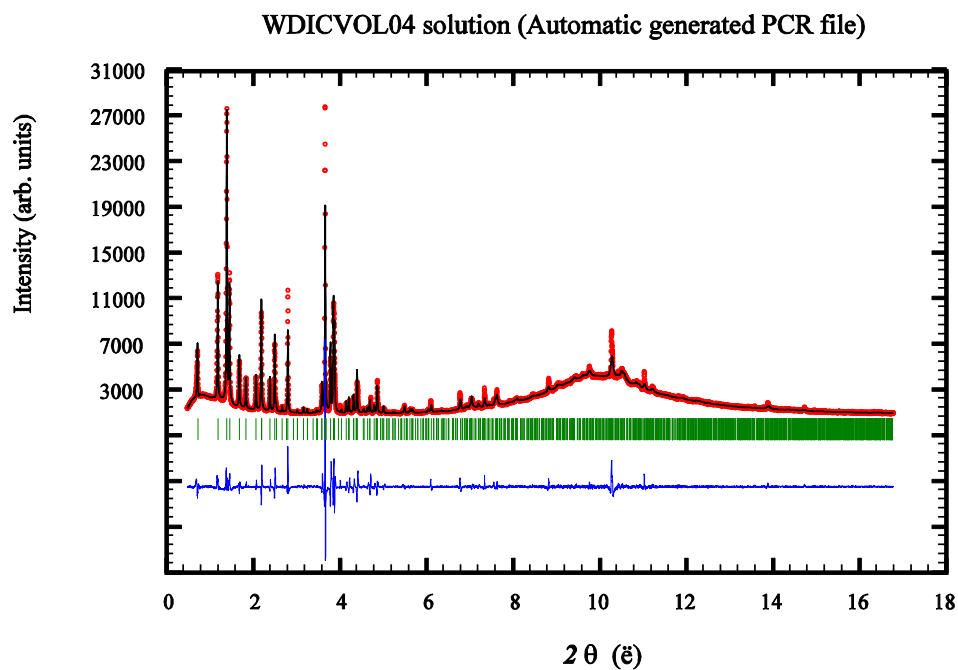


Figure S5. Leball intensity extraction of THF suspended MIL-101(Fe)_NDC (*Fd-3m* *a* = 106.585(6) Rf-factor = 0.35%).

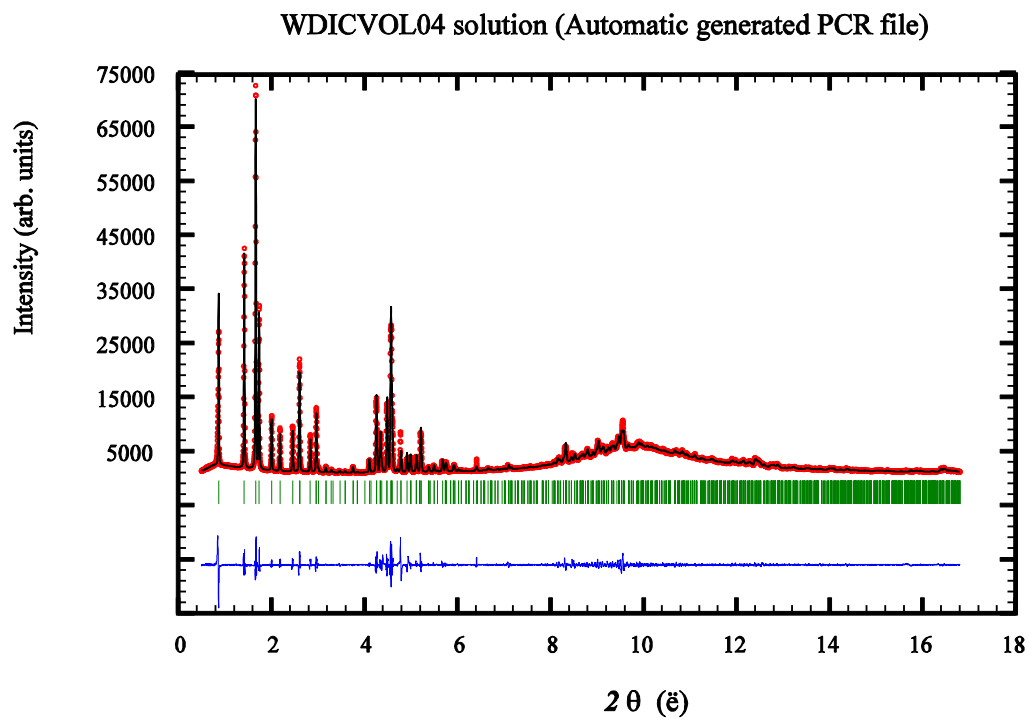


Figure S6. Leball intensity extraction of THF suspended MIL-101(Fe)_BDC ($Fd-3$ $a = 90.196(2)$ Rf-factor = 12.7%).

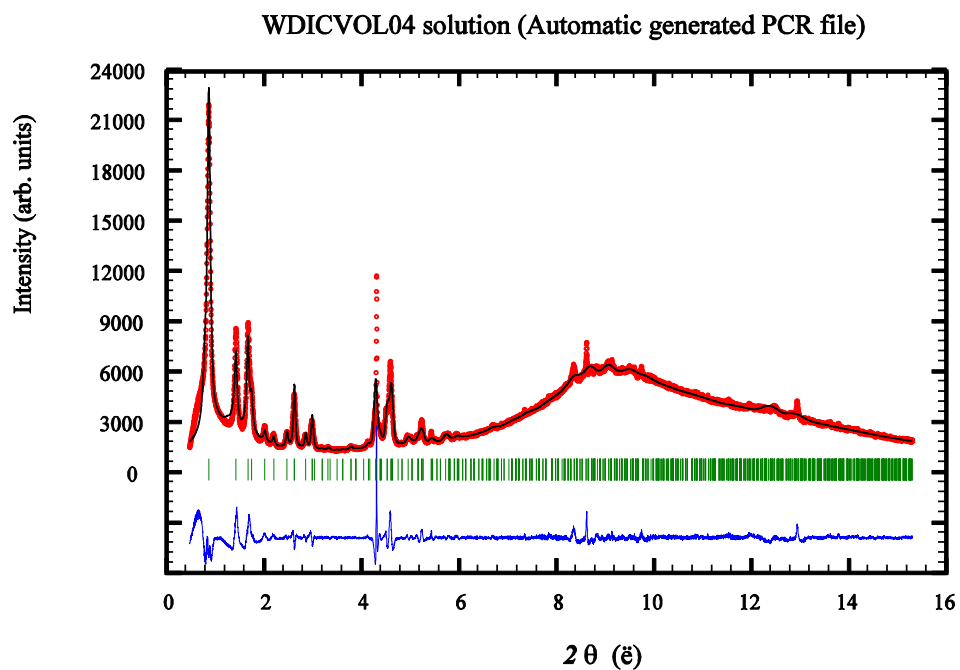


Figure S7. Leball intensity extraction of Tol suspended MIL-101(Fe)_Cl ($Fd-3$ $a = 89.196(17)$ Rf-factor = 1.19%).

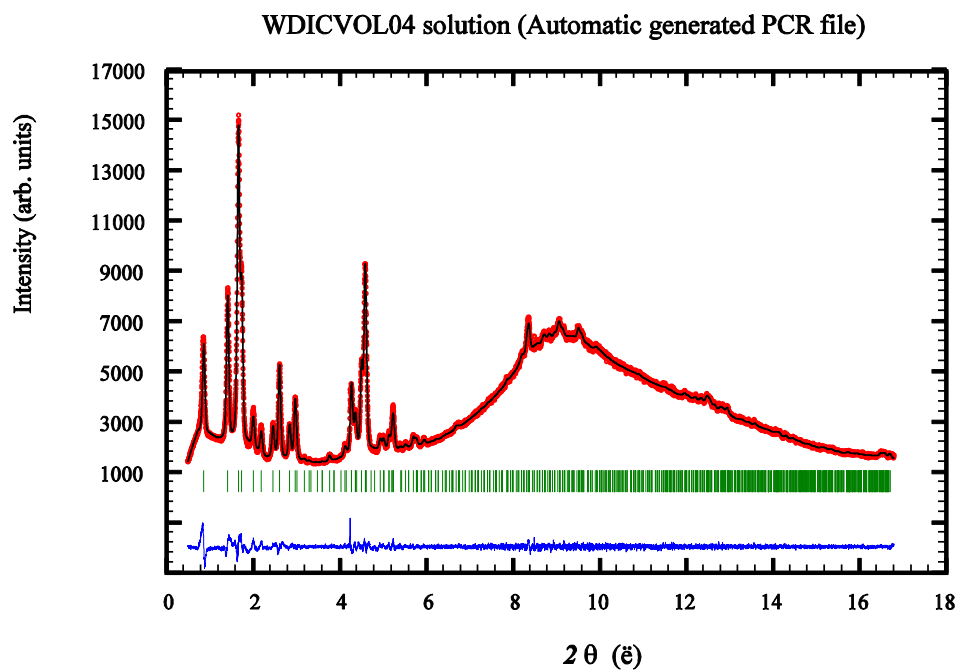


Figure S8. Leball intensity extraction of THF suspended MIL-101(Fe)₂CH₃ (*Fd-3m* $a = 89.646(4)$ Rf-factor = 0.98%).

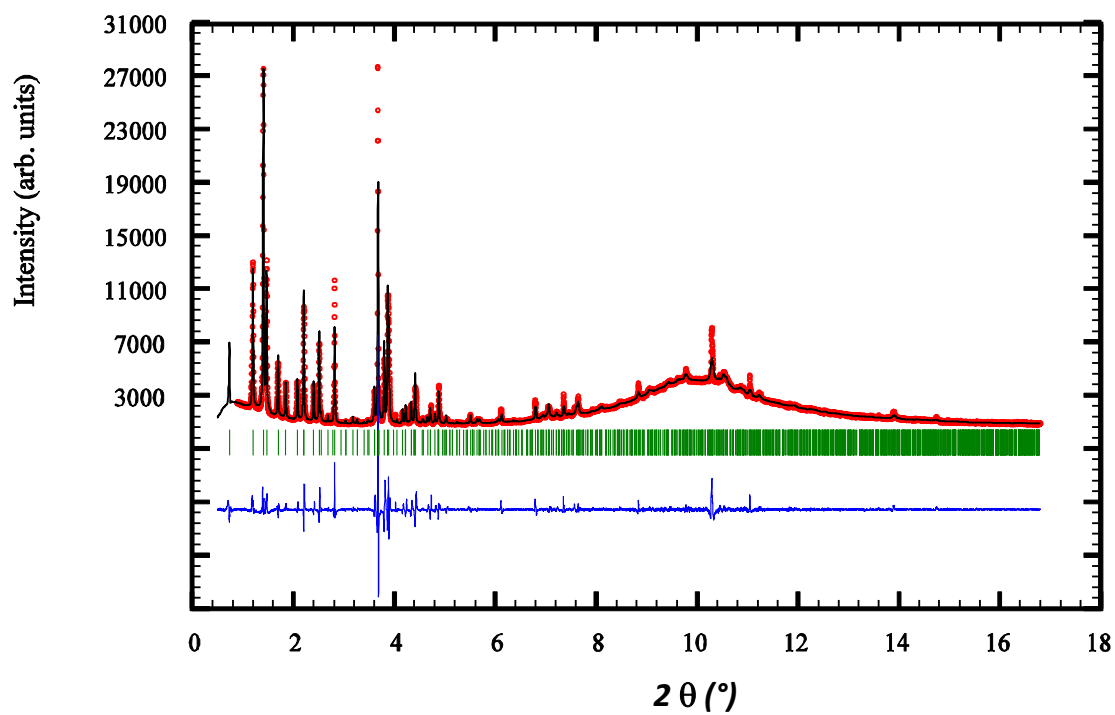


Figure S9. Leball intensity extraction of THF suspended MIL-101(Fe)₂NH₂ (*Fd-3* $a = 89.749(3)$; Rf-factor = 0.52%).

WDICVOL04 solution (Automatic generated PCR file)

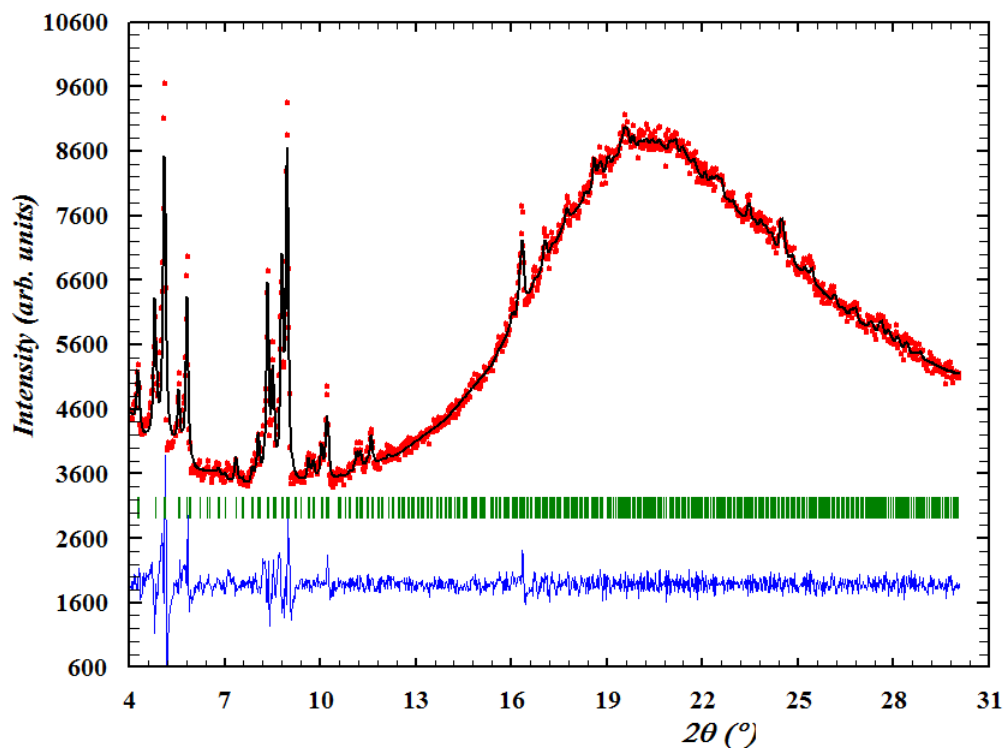


Figure S10. Leball intensity extraction of DMF suspended MIL-101(Fe)_Br ($Fd-3$ $a = 89.87(1)$ Rf-factor = 11.2%).

WDICVOL04 solution (Automatic generated PCR file)

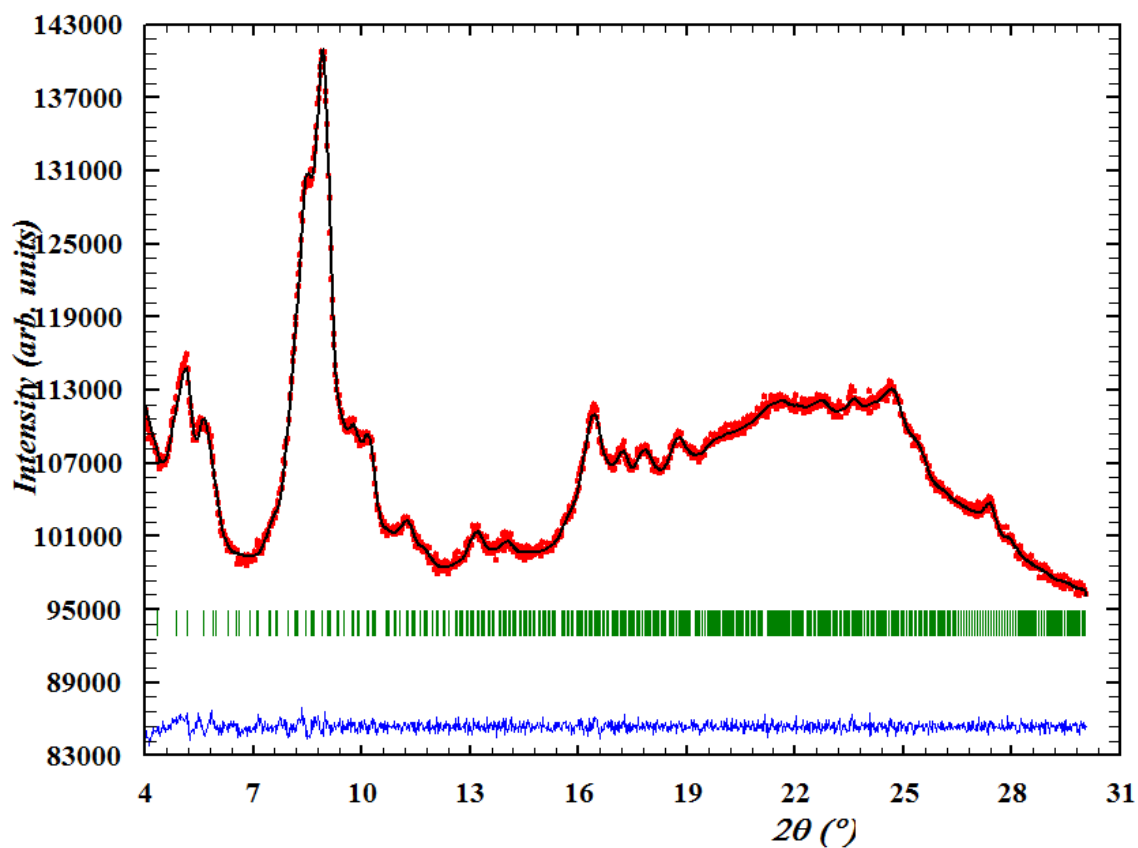


Figure S11. Leball intensity extraction of DMF suspended MIL-101(Fe)_CF₃ ($Fd-3$ $a = 88.84(3)$ Rf-factor = 0.11%).

2.3 STABILITY IN DIFFERENT SOLVENTS BY XRPD

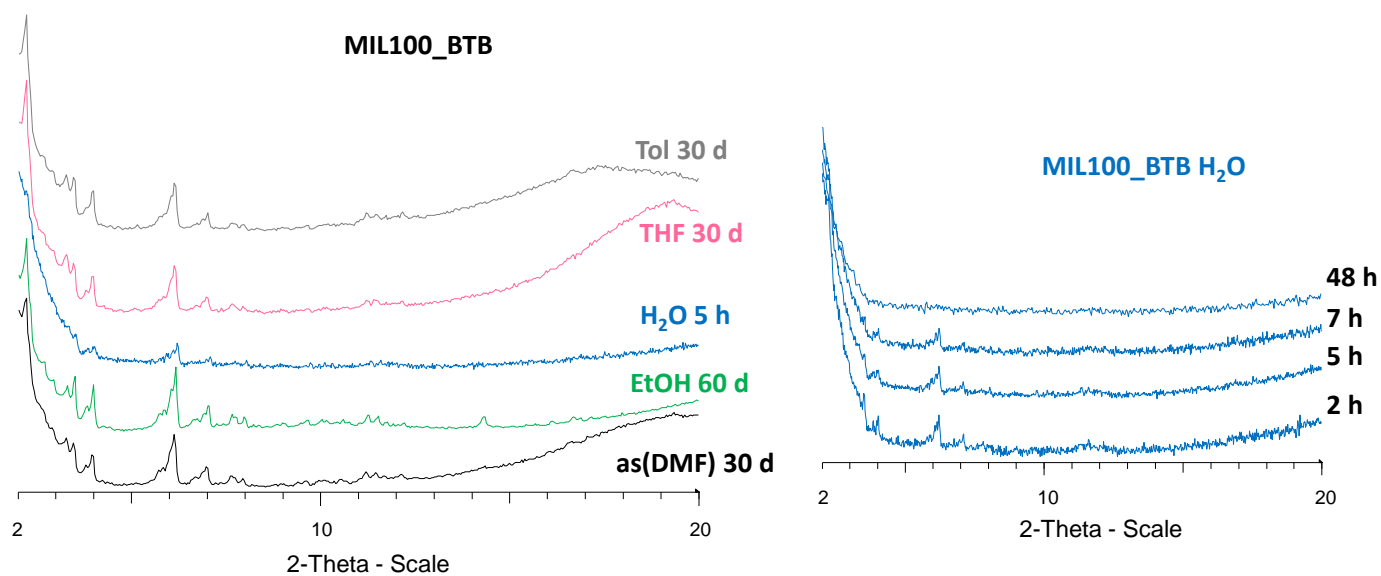


Figure S12. XRPD of MIL-100(Fe)-BTB in different solvents (left) as well as the evolution of the degradation in water as a function of the time (right).

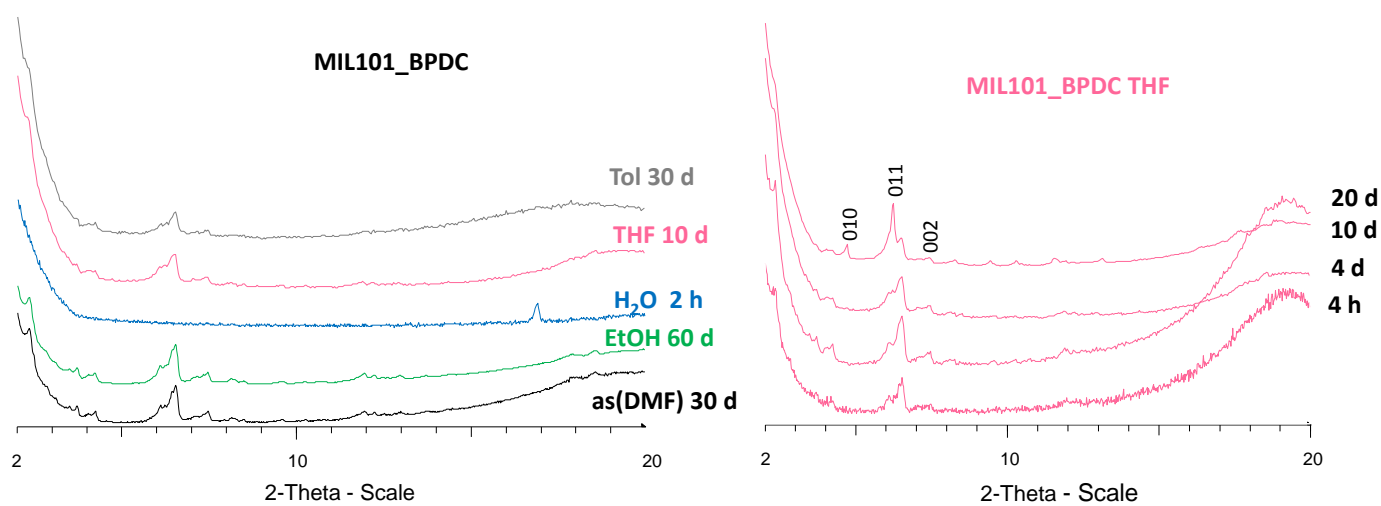


Figure S13. XRPD of MIL-101(Fe)-BPDB in different solvents (left) as well as the evolution of the degradation of the solid in toluene (top right) and THF (bottom right) as a function of the time. Degradation of MIL-101(Fe)-BPDB leads to the formation of an amorphous solid in toluene, whereas in THF the degradation product can be indexed as MIL-88D (hexagonal P62c with $a \sim 20.5$, $c \sim 22.7$ Å; see Miller indices).

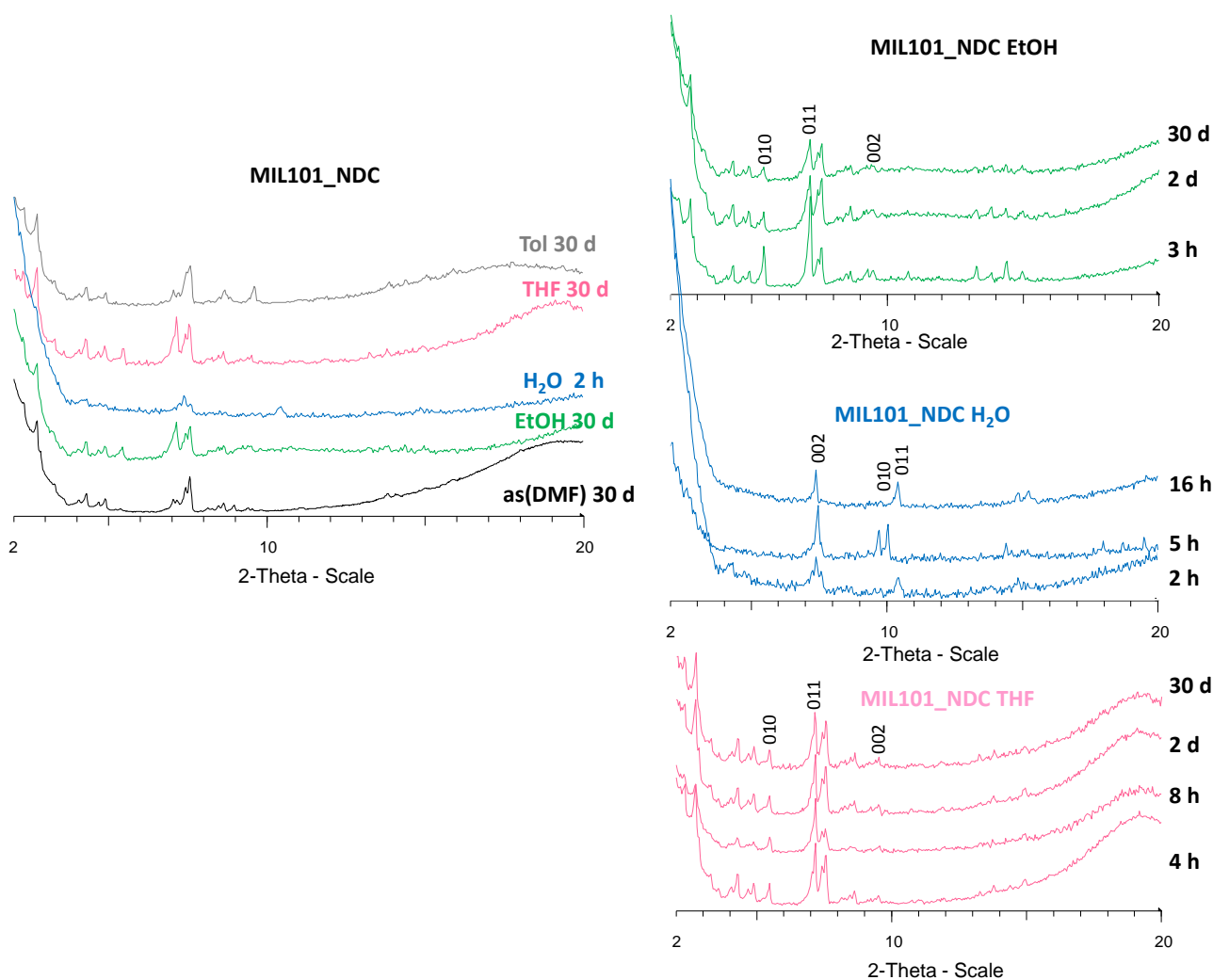


Figure S14. XRPD of MIL-101(Fe)-NDC in different solvents (left) as well as the evolution of the degradation of the solid in ethanol (top right), water (center right) and THF (bottom right) as a function of the time. Degradation of MIL-101(Fe)-NDC leads to the formation a MIL-88C product with different pore openings depending on the solvent, which can be indexed in the hexagonal P62c space group as follows: ethanol and THF $a \sim 18.7$, $c \sim 18.7$ Å and H₂O $a \sim 10.1$, $c \sim 23.1$ Å; see Miller indices).

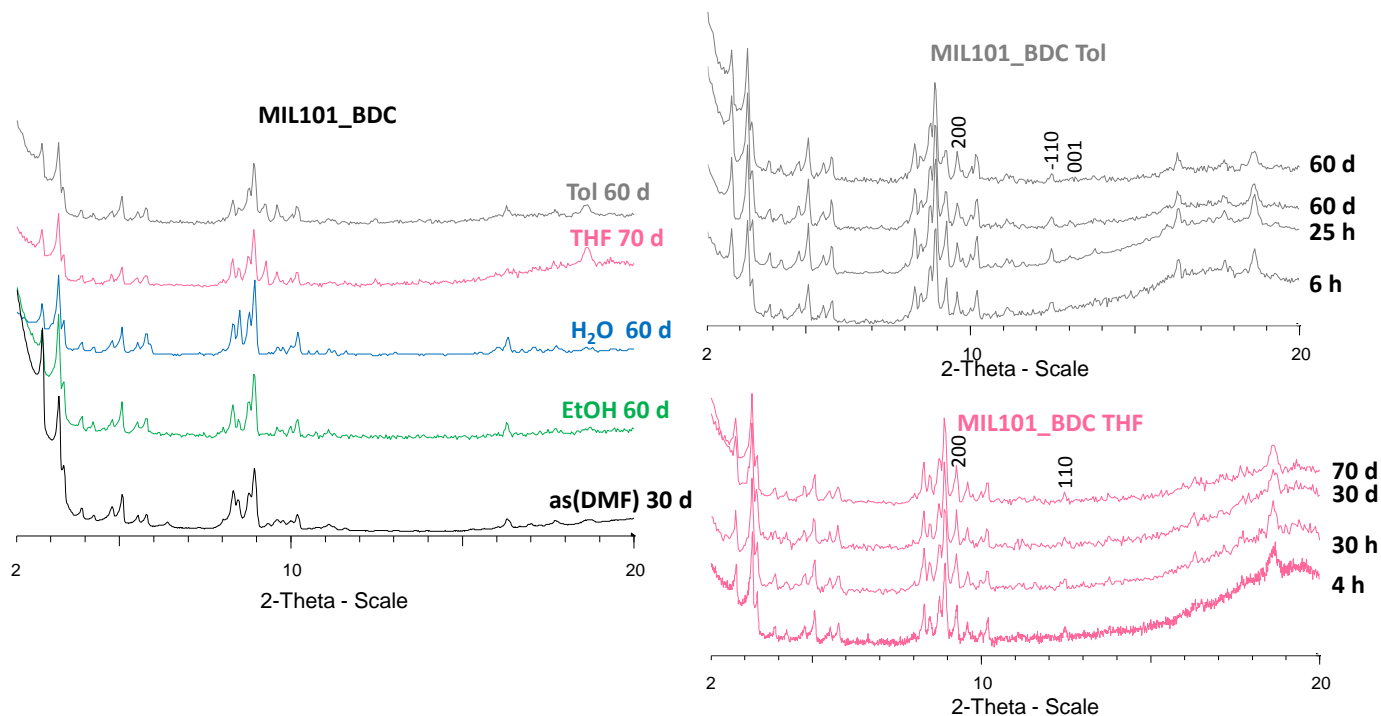


Figure S15. XRPD of MIL-101(Fe)-BDC in different solvents (left) as well as the evolution of the degradation of the solid in toluene (top right) and THF (bottom right) as a function of the time. Degradation of MIL-101(Fe)-BDC leads to the formation a MIL-53 phase. A pattern matching suggests the formation of a monoclinic C2 and C2/c space groups for respectively MIL-101(Fe)-BDC in toluene and THF with the following cell parameters: $a \sim 19.5$, $b \sim 7.5$, $c \sim 6.8$ Å (see Miller indices).

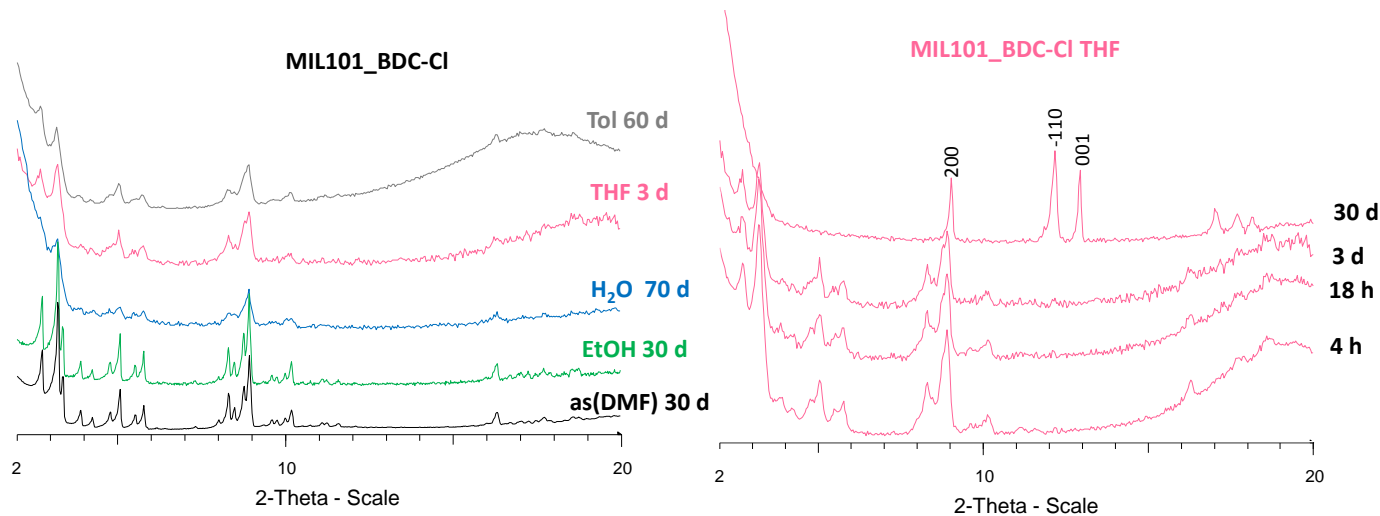


Figure S16. XRPD of MIL-101(Fe)-BDC-Cl in different solvents (left) as well as the evolution of the degradation of the solid in THF (right) as a function of the time. Degradation of MIL-101(Fe)-BDC-Cl leads to the formation a MIL-53 type phase. A pattern matching suggests the formation of a monoclinic C2 space group: $a \sim 19.5$, $b \sim 7.5$, $c \sim 6.8$ Å (see Miller indices).

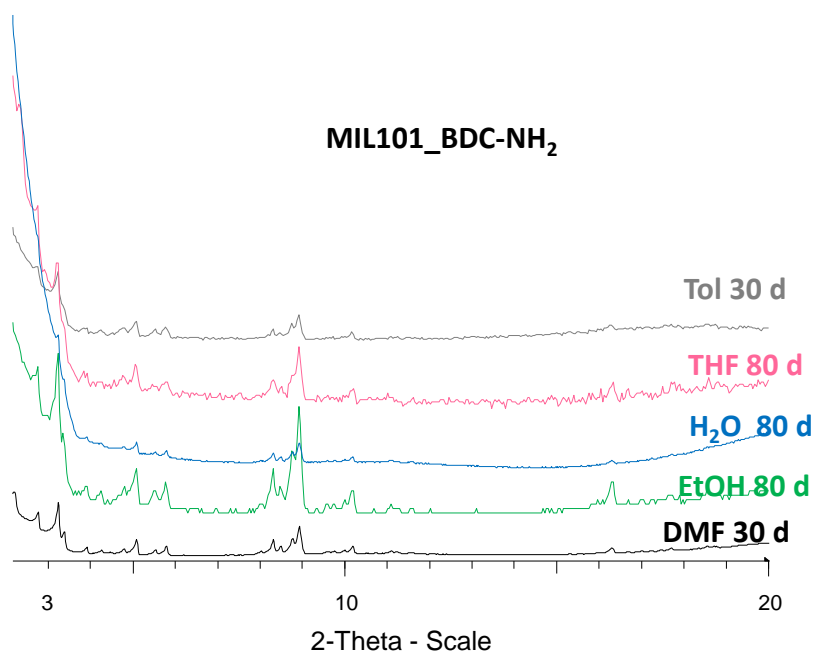


Figure S17. XRPD of MIL-101(Fe)-BDC-NH₂ in different solvents.

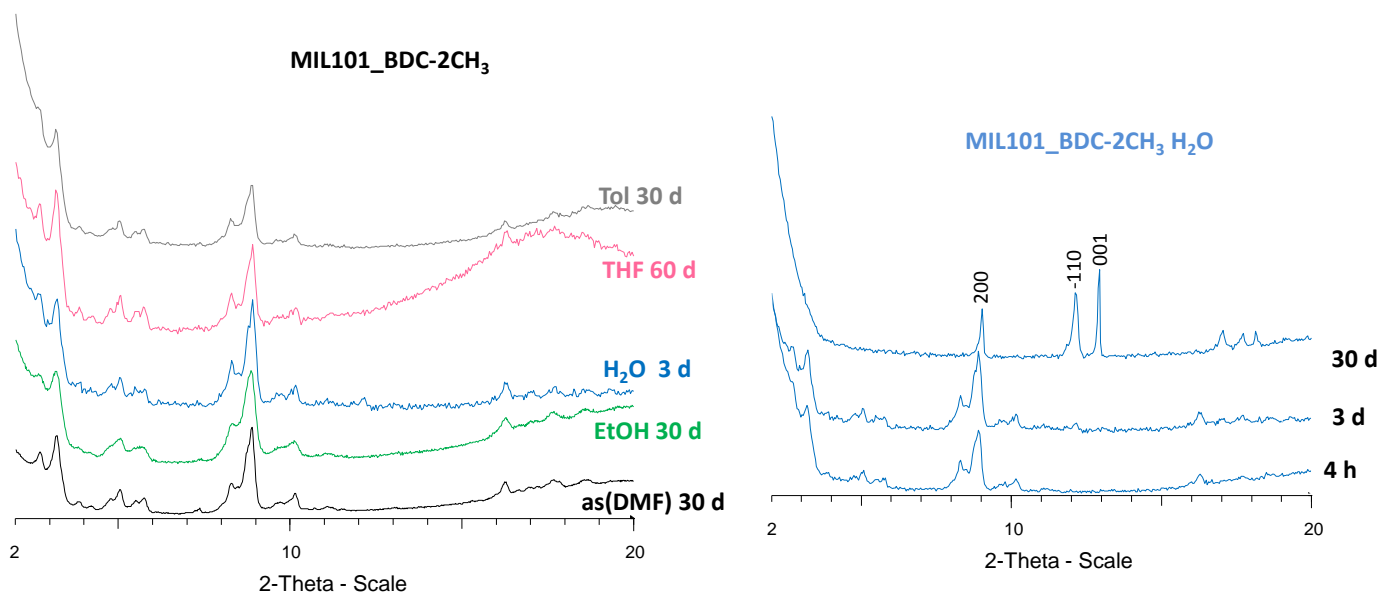


Figure S18. XRPD of MIL-101(Fe)-BDC-2CH₃ in different solvents (left) as well as the evolution of the degradation of the solid in water (right) as a function of the time. Degradation of MIL-101(Fe)-BDC-2CH₃ leads to the formation a MIL-53 type phase. A pattern matching suggests the formation of a monoclinic C2 space group: $a \sim 19.5$, $b \sim 7.5$, $c \sim 6.8$ Å; see Miller indices.

2.4 TGA

Table S1. Chemical composition of the MIL-100/101(Fe)_X obtained by TGA.

MIL100-101_X	% Fe ₂ O ₃ (dry solid)	
	Theoretical	Experimental
BTB	22.7	26.0
BPDC	26.1	30.6
NDC	28.5	31.5
BDC	34.6	34.1
2CH ₃	30.9	31.5
NH ₂	32.5	32.7
Br	25.8	32.6
Cl	30.2	33.3
CF ₃	26.8	30.5

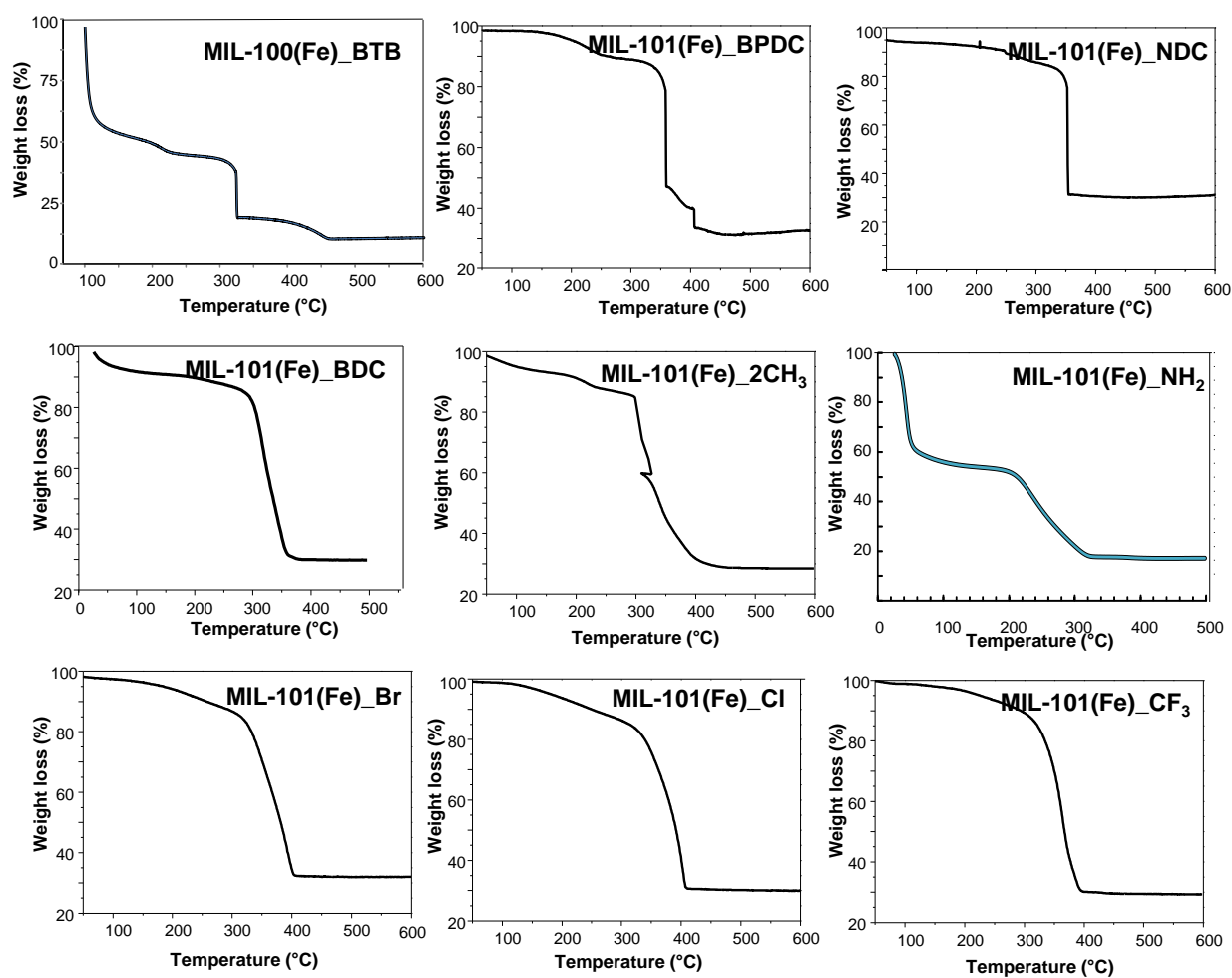


Figure S19. TGA of MIL100/MIL101 NPs.

2.5 N₂ SORPTION MEASUREMENTS

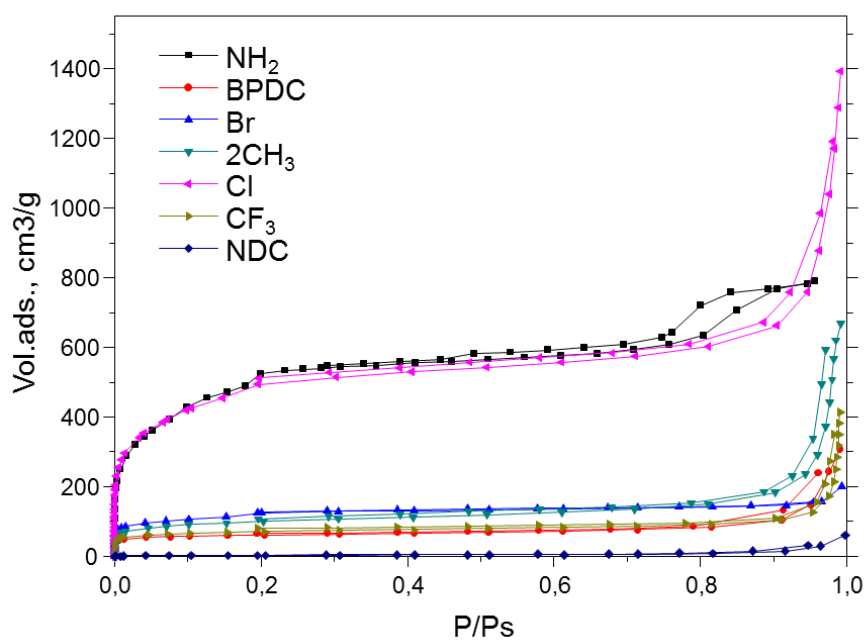


Figure S20. N₂ adsorption/desorption isotherm at 77K of activated MIL-101(Fe)_X nanoparticles.

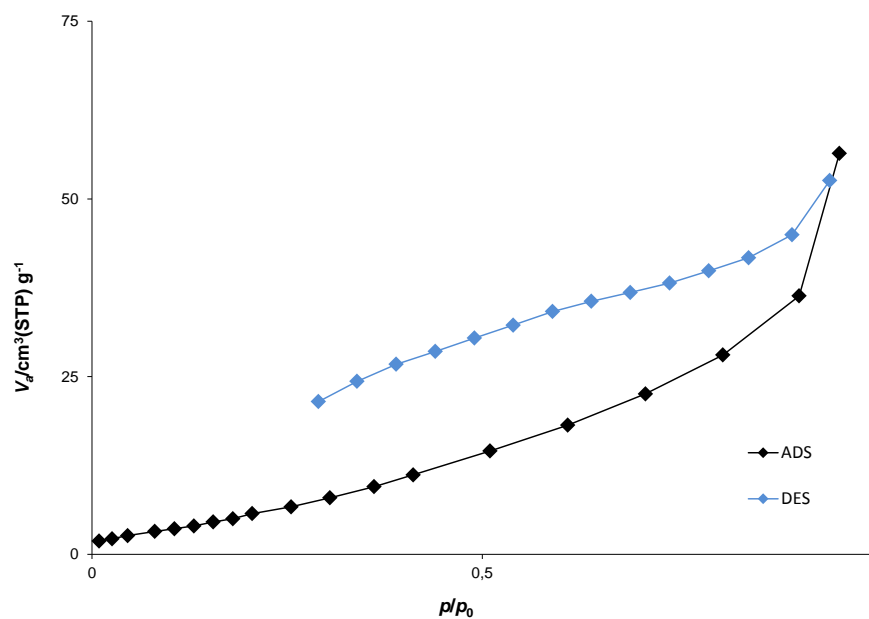


Figure S21. N₂ adsorption/desorption isotherm at 77K of activated MIL-100(Fe)_BTB

Table S2. Experimental and theoretically estimated BET surface area and volume of the MIL-100/101(Fe)s

Linker	$S_{\text{BET}}(\text{m}^2\text{g}^{-1})$		V_p theo. cm^3g^{-1}
	Exp.	Theo.	
BTB	26	3990	3.98
BPDC	210	4500	3.79
NDC	20	3530	2.46
BDC	300	2590	1.76
2CH₃	370	2350	1.49
NH₂	1840	2560	1.62
Br	440	1930	1.25
Cl	1975	2290	1.49
CF₃	245	1820	1.12

2.6 COMPUTING SIMULATION

Simulation-assisted structure determination

The computational effort consisted of determining the structure models for MIL-100(Fe) and the MIL-101(Fe) series. The initial atomic coordinates of the MIL-101 framework was first taken from the refined structure obtained by X-ray diffraction and already published. The starting configurations for each modified MIL-101(Fe)_X (where X= H, Cl, Br, CF₃, NH₂, 2CH₃, biphenyldicarboxylate, naphthalenedicarboxylate) structures were then built by (i) substituting the phenyl rings by the larger linkers or by substituting one H atom of the phenyl ring by the corresponding functionalized groups, and (ii) by imposing the corresponding unit cell parameters obtained from the XRPD refinement. All these models were then energy minimized in the space group determined experimentally by keeping the cell parameters fixed. The optimized structure corresponding to the lowest energy for each modified form was selected. The universal force field (UFF)⁸ for the Lennard-Jones parameters and the charges calculated from the qEq method⁹ as implemented in the Materials Studio software¹⁰ were considered to model the interactions between the whole system. Such a strategy based on the UFF force field has been successfully employed to construct plausible structure of various MILs including the MIL-88(Fe) and MIL-53(Fe) series as well as the different forms of Co(BDP).^{2,11} The Ewald summation was considered for calculating the electrostatic interactions while the short range interactions were evaluated using a cut-off distance of 12 Å. The convergence criteria were set to 1.0×10^{-5} kcal mol⁻¹ (energy), 0.001 kcal.mol⁻¹ Å⁻¹ (forces), and 1.0×10^{-5} Å (displacement) respectively. Similar geometry optimization strategy has been followed for the MIL-100(Fe)_BTB structure using the experimental structure information issued from XRPD, nevertheless the structure has been constructed in *Fd-3* (n°203) then switched back to *Fd-3m* (n°227).

The plausible theoretical structure was determined by the energy criteria. It means that the structure with the lowest energy is chosen while different ligand distributions were tested.

All of the geometry optimizations converged to provide a plausible crystallographic structure for each modified MIL-101 form with the real symmetry.

Geometrical features

Accessible surface area

The accessible surface area of the simulated structure models for MIL-101(Fe) series and MIL-100(Fe)_BTB was estimated using the strategy previously reported by Düren *et al.*¹² This surface was calculated from the center of a nitrogen probe molecule rolling across the surface. While the diameter of the nitrogen probe molecule was considered to be 3.681 Å, the diameters of each atom constituting the MIL-101 structures were taken from the UFF force field.⁸

Free volume

The free volume was calculated for each simulated structure by using a similar method of trial insertions within the entire volume of the unit cell. A probe size of 0 Å was used to enable us to determine this total free volume of the unit cell that is not occupied by the atoms of the framework.¹²

References

- ¹ S.M. Ngola, P.C. Kearney, S. Mecozzi, K. Russell., D.A. Dougherty, *J. Am. Chem. Soc.* **1999**, *121*, 1192.
- ² P. Horcajada, F. Salles, S. Wuttke, T. Devic, D. Heurtaux, G. Maurin, A. Vimont, G. Clet, M. Daturi, O. David, E. Magnier, N. Stock, Y. Filinchuk, D. Popov, C. Rieckel, G. Férey, C. Serre, *J. Am. Chem. Soc.*, **2011**, *133*, 17839.
- ³ Y. Ye, S. A. Künzi, M. S. Sanford, *Org. Lett.*, **2012**, *14*, 4979.
- ⁴ A Boulitif, D. Louer, *J. Appl. Cryst.* **2004** *37*, 724
- ⁵ J-L. Hodeau *et al.*, *SPIE Proceedings*, **1998**, *3448*, 353
- ⁶ J. Rodriguez-Carvajal, T. Roisnel, *International Union for Crystallography*, Newsletter N°20 (May-August) Summer **1998**
- ⁷ Bruker *A X S TOPAS V4.2: General Profile and Structure Analysis Software for Powder Diffraction Data*, **2008**.
- ⁸ A. K. Rappe, C. J. Casewit, K. S. Colwell, W. A. Goddard, W. M. Skiff, *J. Am. Chem. Soc.* **1992**, *114*, 10024.
- ⁹ A. K. Rappe, W. A. Goddard, *J. Phys. Chem.* **1991**, *95*, 3358.
- ¹⁰ *Materials Studio*, v. 5.0, Accelrys, Inc., San Diego, **2009**.
- ¹¹ (a) T. Devic, P. Horcajada, C. Serre, F. Salles, G. Maurin, B. Moulin, D. Heurtaux, G. Clet, A. Vimont, J.-M. Grenèche, B. L. Ouay, F. Moreau, E. Magnier, Y. Filinchuk, J. m. Marrot, J.-C. Lavalley, M. Daturi, G. Férey, *J. Am. Chem. Soc.* **2009**, *132*, 1127; (b) F. Salles, G.

-
- Maurin, C. Serre, P. L. Llewellyn, C. Knofel, H. J. Choi, Y. Filinchuk, L. Oliviero, A. Vimont, J. R. Long, G. Férey, *J. Am. Chem. Soc.* **2010**, *132*, 13782.
- ¹² T. Düren, F. Millange, G. Férey, K. S. Walton, R. Q. Snurr, *J. Phys. Chem. C*, **2007**, *111*, 15350.